Depositional environment of mudflats and mangroves and bioavailability of selected metals within mudflats in a tropical estuary

M. C. Fernandes, G. N. Nayak, A. Pande, S. P. Volvoikar & D. R. G. Dessai

Environmental Earth Sciences

ISSN 1866-6280
Volume 72
Number 6

Environ Earth Sci (2014) 72:1861-1875
DOI 10.1007/s12665-014-3095-y

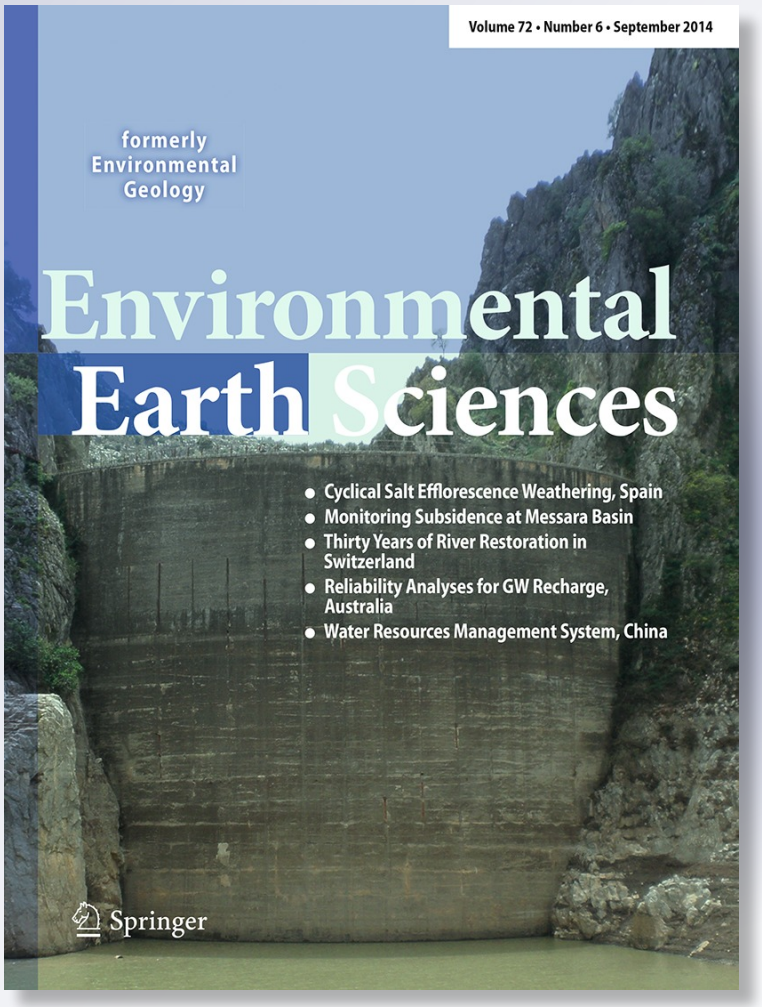

Springer

Environ Earth Sci (2014) 72:1861–1875
DOI 10.1007/s12665-014-3095-y

ORIGINAL ARTICLE

Depositional environment of mudflats and mangroves and bioavailability of selected metals within mudflats in a tropical estuary

M. C. Fernandes · G. N. Nayak · A. Pande · S. P. Volvoikar · D. R. G. Dessai

Received: 7 February 2013 / Accepted: 25 January 2014 / Published online: 14 February 2014

Abstract Four sediment cores representing adjacent mudflat and mangrove sub-environments of middle estuary (Shastri) were analyzed for sand, silt, clay, and organic carbon. Total metal concentration of iron (Fe), manganese (Mn), nickel (Ni), zinc (Zn), chromium (Cr), copper (Cu), cobalt (Co), and lead (Pb) and chemical speciation of Fe, Mn, and Co on selected samples was also carried out on mudflat cores. The sediments in the upper middle estuary were found to be deposited under highly varying hydrodynamic energy conditions; whereas lower middle estuary experienced relatively stable hydrodynamic energy conditions with time. The tributary joining the river near the upper middle estuary is found to be responsible for the addition of enhanced organic carbon and metal concentrations. Speciation study indicated Fe and Co are from natural lithogenic origin while Mn is derived from anthropogenic sources. Higher Mn and Co than apparent effects threshold can pose a high risk of toxicity to organisms associated with these sediments.

Keywords Sediment · Metal · Tropical estuary · Bioavailability

M. C. Fernandes · G. N. Nayak (✉) · A. Pande · S. P. Volvoikar
Marine Sciences Department, Goa University, Taleigao, Goa 403206, India
e-mail: nayak1006@rediffmail.com; gnnayak@unigoa.ac.in

D. R. G. Dessai
National Center for Antarctic and Ocean Research, Headland Sada, Vasco da Gama, Goa 403804, India

Introduction

Estuaries, the transition zones between marine and terrestrial environments, are classified into three distinct zones: inner river-dominated zone, central zone where river flow is countered by flood-tidal energy and outer marine zone which is dominated by waves and/or tides (Dalrymple et al. 1992). The boundaries between the three transition zones vary with tides, season, and weather (Fairbridge 1980). Estuary receives sediments from different sources which include fluvial, marine, atmosphere, and mixtures (Wu et al. 2011). In general, sediments within outer zone represent developing of tidal bar-channel complexes, tidal flats, lagoons, and salt marshes (Dalrymple et al. 1992). Low-energy central zone facilitates deposition of large quantity of finer sediments (Dalrymple et al. 1992). Mudflats and mangroves are adjacent sub-environments along estuarine tidal flats in tropical region (Harbison 1986; Wells and Coleman 1981). Mudflats cover large nonvegetated areas that are exposed during low tide and submerged during high tide (Reineek 1972). Mangroves, on the other hand, are salt-tolerant shrubs and trees associated with a unique horizontal root network (Soto-Jime'nez and Pa'ez-Osuna 2001; Kumaran et al. 2004). They primarily consist of fine sediment deposits (<63 μm) and are influenced by tides, waves and fluvial processes (Lesueur et al. 2003; Dalrymple et al. 1992; Allen and Posamentier 1993). Along with finer sediments, these sub-environments favor deposition of higher organic matter. These fine cohesive sediments favor the accumulation of metals (Cundy and Croudace 1995; Spencer et al. 2003; Szefer et al. 1995; Delacerd 1983). Metals have great ecological significance because of their toxicity, persistence and bioaccumulation capacity (Klavinš et al. 2000; Tam and Wong 2000). Metals cannot be biologically or chemically degraded (Marchand et al. 2006). Understanding abundance and distribution of

metals in mudflats and mangroves sediments is, therefore, important as they are key habitats for a number of macrofaunal species and act as important food sources or nursery grounds for fish communities (Boyes and Allen 2007) and also has potential to harm human health via the food chain (Hu et al. 2013). Mudflats and mangroves are extensive along central west coast of India. Attempts have been made to understand these depositional environments and metal distribution in recent years by number of researchers (Singh and Nayak 2009; Fernandes and Nayak 2009, 2012a, b; Siraswar and Nayak 2011; Fernandes et al. 2011; Pande and Nayak 2013a, b; Volvoikar and Nayak 2013a, b, c; Singh et al. 2012, 2013). However, these studies are mainly based on total metal concentration and do not reflect the mobility and potential availability for biota. The mobility of metals associated with different sedimentary fractions is in the order: exchangeable > carbonate > Fe–Mn oxide bound (reducible) > organic and sulfide bound (oxidizable) > residual. Metals bound to different phases respond differently in the sedimentary and diagenetic environment, and thus have different potentials for remobilization and for the uptake by biota (Jones and Turki 1997). The determination of geochemical associations of metals thus provide useful information concerning the origin, absolute levels, mobilization, mode of occurrence and biological availability of metals (Thomas and Bendell-Young 1998; Almas et al. 2006; Dessai and Nayak 2009). In this paper an attempt is made to study the distribution and abundance of sediment components, organic carbon and selected elements in sediments with time within the middle estuary to understand the depositional environment, post depositional processes and bioavailability of metals.

Materials and methods

Study area

The Jaigad creek is fed by the Shastri River which originates in the Western Ghats, follows a meandering course and opens into the Arabian Sea (Fig. 1a, b). The total length of the river is about 64 km. The adjoining promontory at the mouth has Jaigad Port. For the proximal 26 km the river flows through a steep mountainous region. There are several small tributaries which join Shastri estuary namely Gad, Kapshi, and Bav (Fig. 1a). The catchment area consists of Deccan basalts which are known to contain higher concentration of elements such as Fe, Co, Cu, etc. (Rajamanickam and Gujar 1995). The river is influenced by tides up to 45 km from the mouth (Achuthankutty et al. 1981). Shastri estuary falls under mesotidal category (Davies 1964) with the average spring tidal range of approximately 2.8 m (Singh 2013).

Sampling and analysis

Four shallow cores were collected from the Shastri estuary using hand driven PVC coring tube. Two cores represented mudflats; namely S9 (Guhajan) and S17 (Mendegaon) and the other two were from the adjacent mangroves viz. S11 (Guhajan) and S22 (Mendegaon), respectively (Fig. 1a). The core length varied from 44 cm (S17) to 112 cm (S9) for mudflat core and 40 cm (S22) to 70 cm (S11) for mangrove core. Core S9 and S11 represented the lower middle estuarine region whereas S17 and S22 represented the upper middle estuarine region. In the field, cores were sub-sampled at 2 cm interval with the help of a plastic knife, transported to laboratory in ice box, frozen at 4 °C and later oven-dried at 60° C. Sediment components (sand:silt:clay) were analyzed by pipette method (Folk 1968). Organic carbon was determined using the Walkey-Black method (1947), adopted and modified from Jackson (1958). All the sub-samples of mudflat cores were digested with HF, HNO_3 and $HClO_4$ acid mixture for total metal analyses. The metals viz. Fe, Mn, Ni, Cr, Cu, Zn, Co and Pb were analyzed using Atomic Absorption Spectrophotometer (Varian AAS 240FS model). Together with the samples, certified reference standards from the MAG-1 (Marine mud) and GR-1 (Green River sediment) were digested and run, to test the analytical and instrument accuracy of the method. The average recoveries were around 90–97 %. Suitable internal chemical standards (Merck Chemicals) were used to calibrate the instrument. Also recalibration check was performed at regular intervals. The geochemical data of the post archean average shale given by Turekian and Wedepohl (1961) were used as the background for the computation of index of geoaccumulation (I_{geo}). A modified sequential extraction procedure (Tessier et al. 1979) was employed for the selected sub-samples of mudflat cores in order to evaluate speciation of metals (Fe, Mn, and Co). The procedure involves extraction of five phases, viz., exchangeable phase, carbonate phase, Fe–Mn oxide phase, organic matter/sulfide bound phase, and the residual phase. Further, to understand the potential bioavailability or the risk of toxicity of the studied metals to the biota, the average concentration of metals obtained after total acid digestion as well as sequentially extracted bioavailable fractions (i.e., sum of exchangeable, carbonate, Fe–Mn oxide and organic bound) was compared with the sediment quality values (SQV) following screening quick reference table (SQUIRT). SQUIRT was developed by NOAA for screening purposes. Based on SQUIRT, the guideline values are categorized into five classes following Buchman (1999) which elucidate the toxicity level of the metals. The implication of SQV is to achieve the information on toxicity of metals to the biota and thus understand the impact on environment

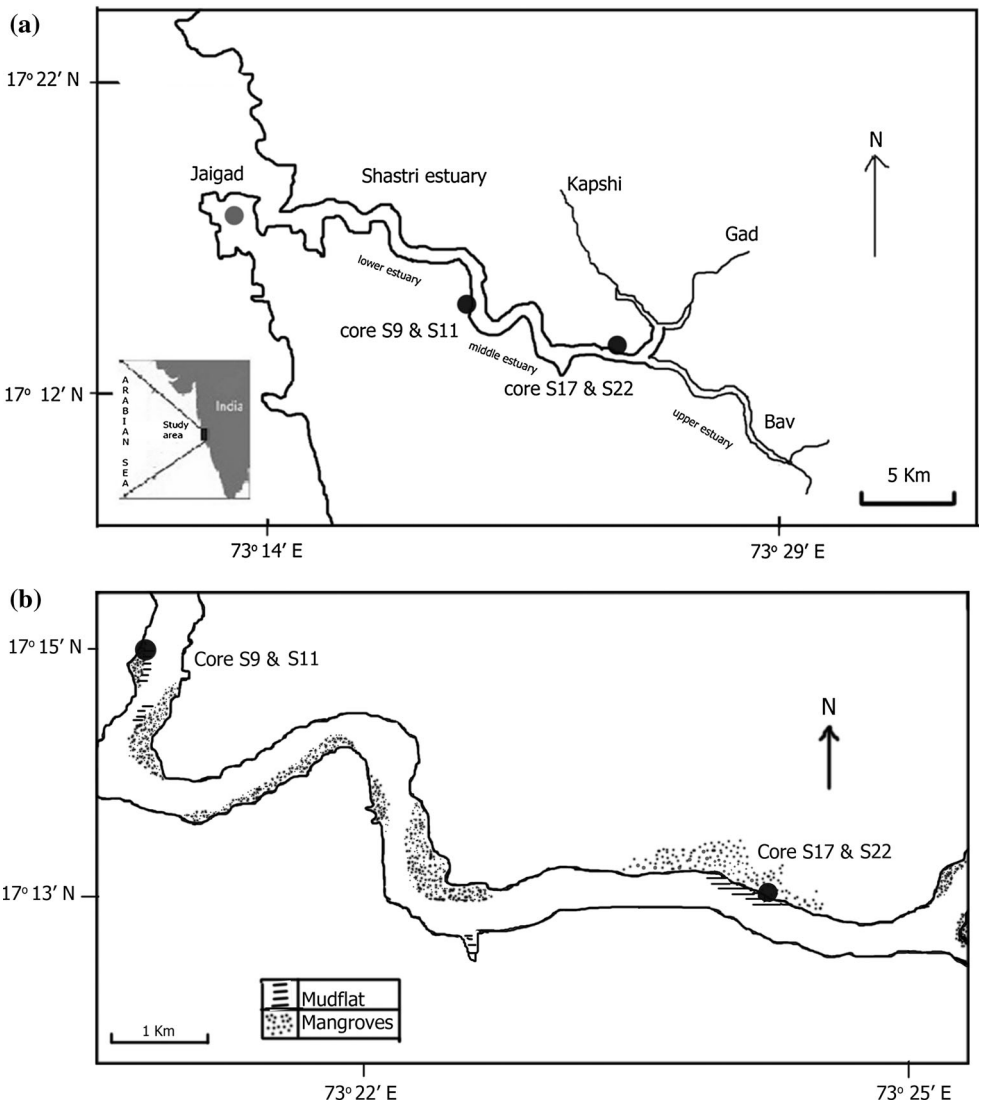

Fig. 1 **a** Map showing locations of sediment core collection in the Shastri estuary. **b** Map showing the mudflats and mangroves along middle Shastri estuary

(Spencer and MacLeod 2002; Attri and Kerkar 2011). Correlation was obtained between the different parameters using the computer software STATISTICA (Statsoft 1999).

Results and discussion

Spatial and temporal distribution of sediment components and organic carbon

In mudflat core S9 (Fig. 2a), sand content varies from 9.18 to 22.95 % whereas silt and clay content varies from 45.37 to 68.59 % and 18.28 to 36.20 %, respectively, with mean values for sand, 15.47 %; silt, 54.78 % and clay, 29.75 %. Organic carbon content varies from 1.46 to 3.07 % with its mean value 1.88 %. In mudflat core S17 (Fig. 3a) sand varies from 2.90 to 34.33 % whereas silt, clay and organic carbon vary from 40 to 69.40 %, 11.16 to 41.72 % and 1.37 to 3.32 %, respectively, with mean values of sand, 16.72 %; silt, 54.95 %; clay, 28.33 % and organic carbon, 2.36 %.

In Mangrove core S11 (Fig. 4), sand varies from 9.86 to 19.72 % whereas silt, clay and organic carbon vary from 40.06 to 64.57 %, 21.28 to 45.36 % and 1.15 to 2.35 %, respectively, with mean values of sand, 14.73 %; silt, 48 %; clay, 38 % and organic carbon, 1.40 %. In Mangrove core S22 (Fig. 5) sand component ranges from 4.93 to 50.71 % whereas silt, clay and organic carbon range from 32.97 to 66.27 %, 15.40 to 36.04 % and 0.87 to 2.27 %, respectively, with mean values of sand, 20.98 %; silt, 52.12 %; clay, 26.91 % and organic carbon, 1.90 %.

At lower middle estuary, silt was noted to be relatively higher in mudflat sediments (core S9) while clay was higher in mangrove sediments (core S11). However, mud

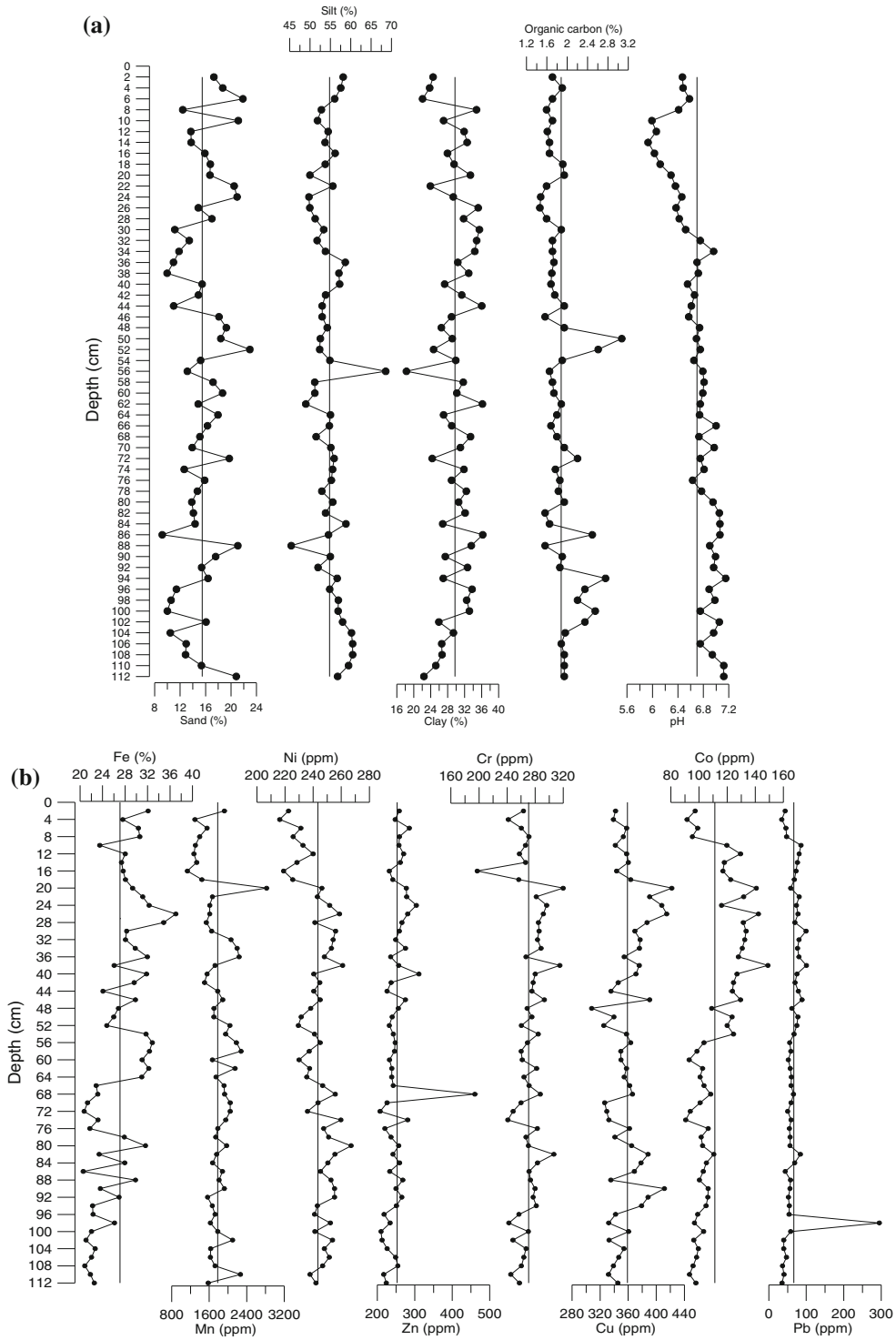

Fig. 2 **a** Vertical profile of sediment components and organic carbon with depth in mudflat core S9 (location: Guhajan, lower middle estuary). **b** Vertical profile of metals viz. Fe, Mn, Ni, Zn, Cr, Cu, Co, and Pb in sediment with depth in mudflat core S9

content (silt + clay) was maintained higher in mangrove sediments as compared to mudflat. Not much difference in the distribution of sand and organic carbon was noted between mudflat and mangrove sediments at this location. Towards the upper middle estuary, sand was relatively higher in mangrove sediments (core S22) as compared to mudflat (core S17). This may be the result of presence of coarse calcareous sand, calcareous muddy gastropods shells, bivalves, etc. (Welle et al. 2004) which are dominant in mangroves than in mudflats. Lower organic carbon percentage was observed in mangrove core S22 as compared to mudflat core S17.

Low fluvial discharge and a better mixing of saline and fresh water are known to facilitate flocculation and settling of

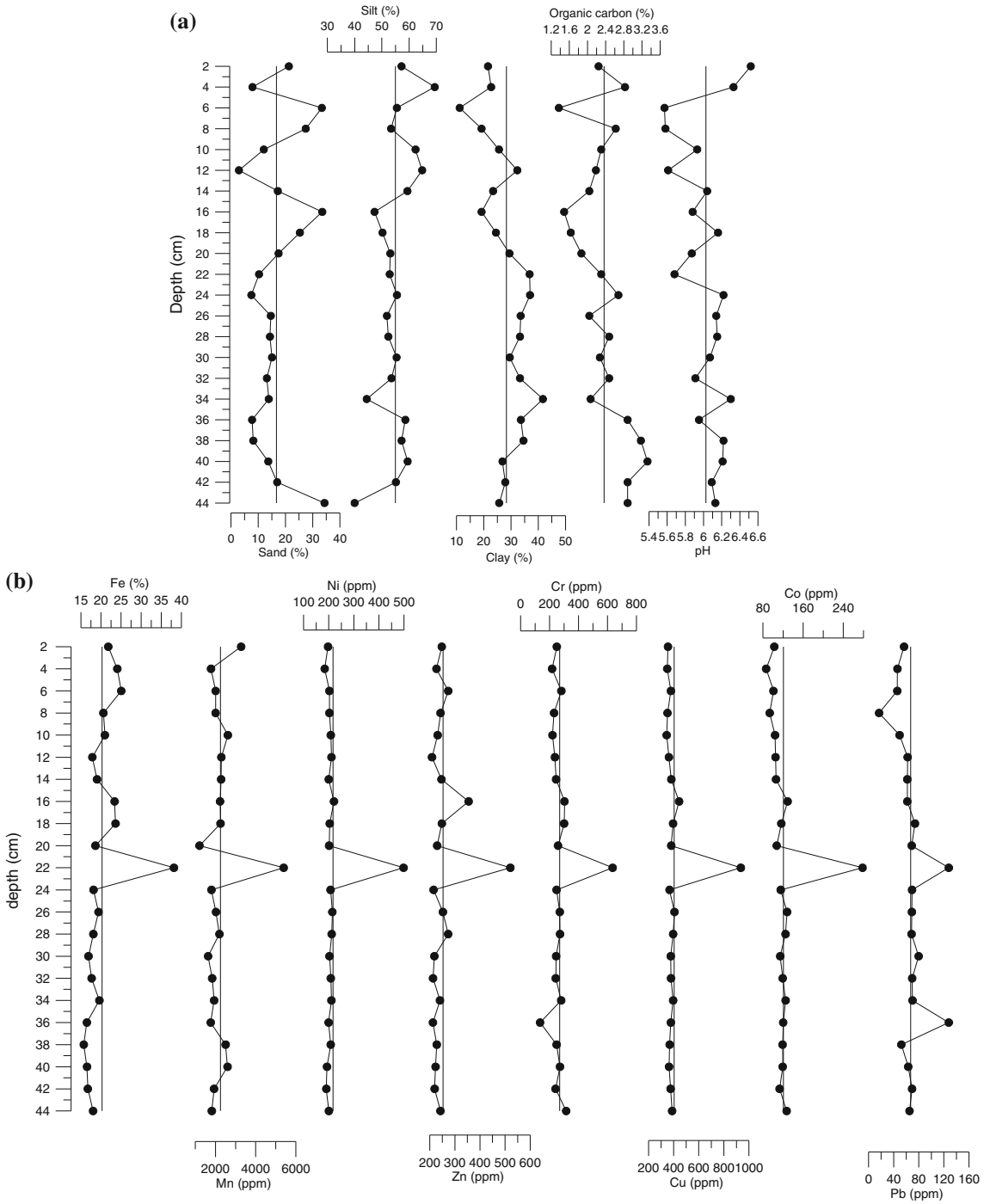

Fig. 3 **a** Vertical profile of sediment components and organic carbon with depth in mudflat core S17 (Location: Mendegaon, upper middle estuary). **b** Vertical profile of metals viz Fe, Mn, Ni, Zn, Cr, Cu, Co, and Pb in sediment with depth in mudflat core S17

finer particles (Nair et al. 1993). This process, therefore, explains the deposition of relatively lower sand and higher mud (i.e., silt + clay) content within mudflat and mangrove cores (core S9 and S11) collected from lower middle estuary as compared to cores collected from the upper middle estuary (core S17 and S22). Organic carbon, however, showed higher percentage in mudflat and mangrove cores of the upper middle estuary as compared to the lower middle estuary. The tributary joining the river little upstream side of the sampling location of cores S17 and S22 is probably responsible for the deposition of the observed coarser sediments and higher organic carbon content within the upper middle estuary.

In mudflat core S9, sand and clay profiles showed a fluctuating trend along the average line, while silt showed

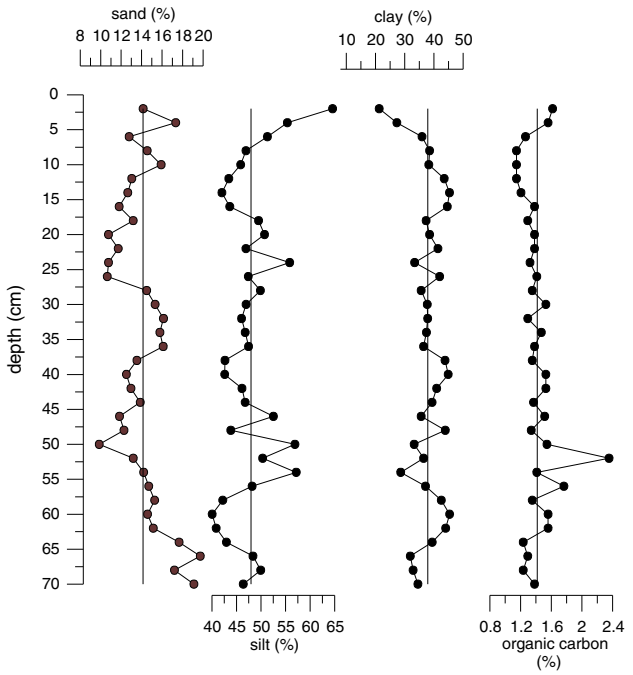

Fig. 4 Vertical profile of sediment components and organic carbon with depth in mangrove core S11 (Location: Guhajan, lower middle estuary)

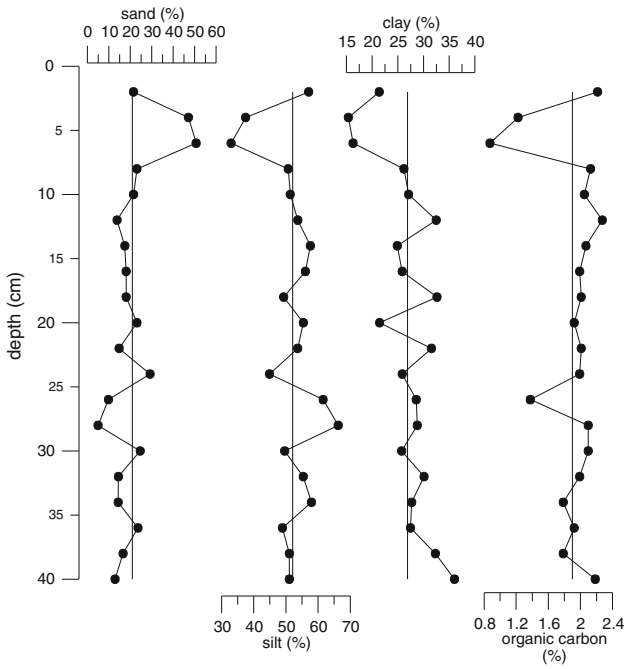

Fig. 5 Vertical profile of sediment components and organic carbon with depth in mangrove core S22 (Location: Mendegaon, upper middle estuary)

almost constant trend (Fig. 2a). However, slightly higher values for silt were noted towards the bottom and surface of the core with a peak value at 56 cm depth. Organic carbon profile also showed a constant trend with a prominent peak at 50 cm depth. In mudflat core S17, not much variation was noted for sand below 20 cm depth except a high value at 44 cm. Above 20 cm depth sand showed large fluctuating trend. Silt and clay compensated for the variation in sand percentage. Similarity in the distribution pattern of finer sediment components, i.e., silt and clay were noted above 32 cm depth. The distribution pattern of sediment components within the upper 20 cm may be due to the variations in fluvial input in recent years. The distribution of organic carbon showed similarity with silt and clay components, indicating association of organic carbon with finer sediment components (Mayer and Xing 2001) and the pH gradually decreases towards the surface in both the cores.

In mangrove core S11 it is noted that there is an increase in silt percentage in recent years. Clay shows opposite distribution pattern to that of silt all along the length of the core. Organic carbon distribution was similar to that of clay below 38 cm and to that of silt above 38 cm indicating their association. In mangrove core S22 large increase in sand percentage was noted above 8 cm depth. Silt compensated for the variation in sand percentage from bottom to the surface of the core. Clay percentage decreased considerably from bottom to surface and showed similarity in distribution pattern with that of silt. Organic carbon distribution was similar to that of silt and clay. The higher concentration of organic carbon towards the bottom of core S17 and to some extent core S22, corresponding with lower sand content, suggested deposition of organic matter together with finer sediments under calm conditions which were probably prevalent in the past (Francois 1988; Kumar and Edward 2009).

Hydrodynamics

To understand the hydrodynamic conditions of depositional environment, ternary diagram proposed by Pejrup (1988) is plotted. Ternary diagram by Pejrup (1988) modifies and expands Folk's diagram (1968) on the basis of hydrodynamic conditions. The lines separating the four hydrodynamic groups, being used to highlight the energy gradient from lower (clay-dominated mud) to higher energy levels (silt dominated mud) (Fig. 6). Pejrup (1988) has interpreted that section I indicates very calm hydrodynamic conditions rarely found in estuaries and sections II to IV indicate increasingly violent hydrodynamic conditions. Plots (Fig. 6) reveal that sediments must have deposited under relatively violent hydrodynamic conditions. However, in case of core S11 collected from the lower middle estuary, some points were also observed in group II (C) indicating that these sediments were deposited under relatively calm to relatively violent hydrodynamic energy conditions. It is important to note here that the data plots of mudflat and

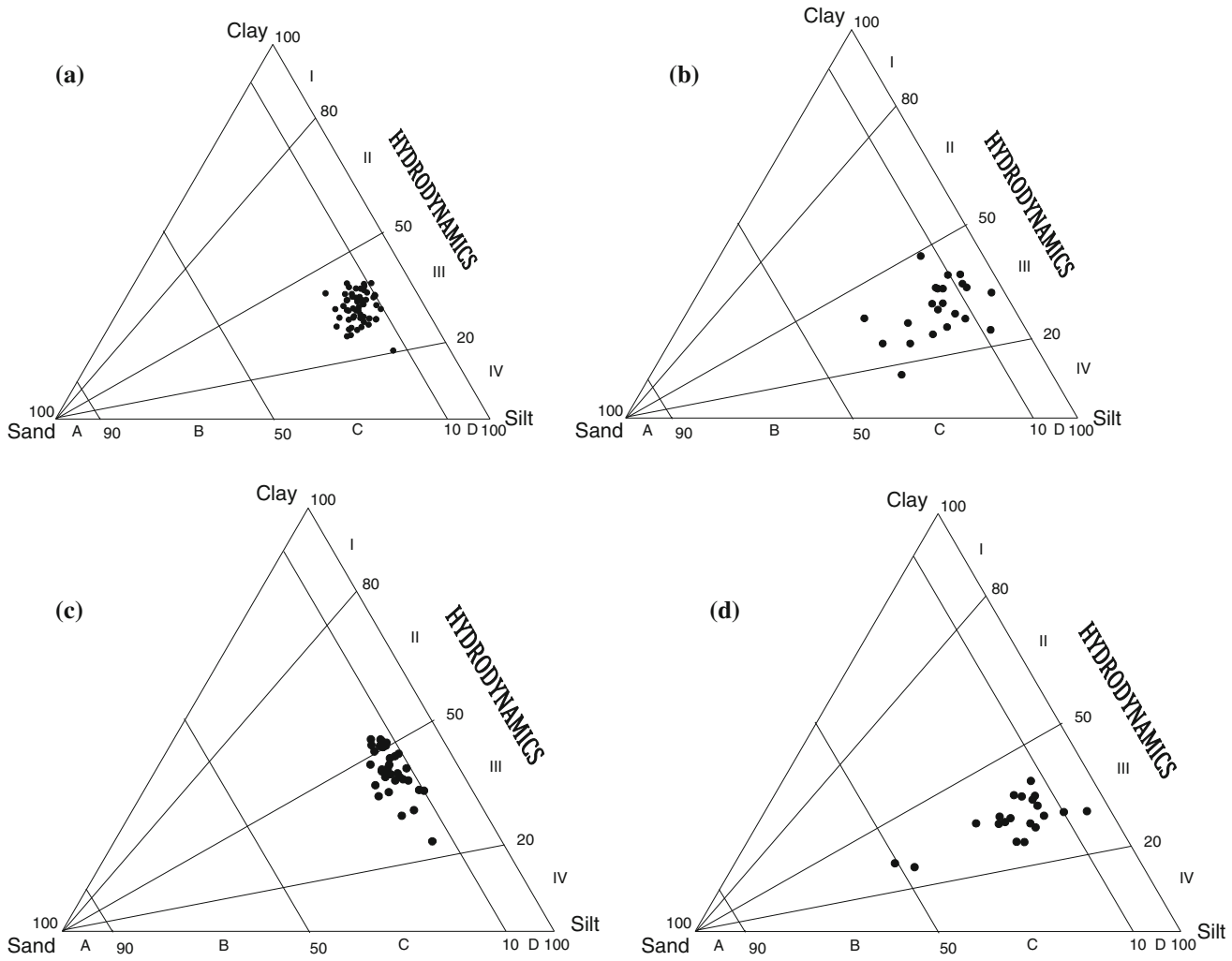

Fig. 6 Triangular diagram for sand–silt–clay with various grades of hydrodynamic condition for core **a** S9, **b** S17, **c** S11, **d** S22, after Pejrup (1988)

mangrove cores collected from the upper middle estuarine region are more spread over indicating larger variation in energy conditions at this location when compared to the lower middle estuarine region.

Metal geochemistry

Distribution of iron and manganese

In core S9 (Fig. 2b), Fe varies from 21.00 to 37.00 % (avg. 27 %) and Mn ranges from 1,133 to 2,824 ppm (avg. 1,778 ppm). Fe showed almost constant trend from bottom up to 100 cm depth. This is followed by a fluctuating increasing trend up to 80 cm and a decreasing trend up to 76 cm depth. Above 76 cm Fe maintained constant trend up to 66 cm. Increase in Fe concentration was observed between 66 and 52 cm depth. Between 52 and 26 cm depth Fe showed fluctuating increasing trend with a peak value at 26 cm. A gradual decrease in Fe concentration up to 16 cm depth was noted, this is followed by a slight increasing trend up to the surface of the core. Mn showed almost constant trend from bottom to 38 cm. Between 36 and 4 cm a gradual decrease in Mn concentration is noted except a higher peak value of 2,824 ppm at 20 cm depth. At the surface slight increase in Mn concentration similar to that Fe is noted. When the distribution patterns of Fe and Mn were compared, both the metals showed a decrease in concentration within the upper 22 cm. The presence of strong Fe and Mn peaks at 26 and 20 cm depth indicated redox mobilization and re-precipitation of these metals in the form of oxides and hydroxides (McCaffrey and Thomson 1980; Zwolsman et al. 1993). Under oxidizing conditions insoluble Fe and Mn oxides are formed. Under suboxic conditions, the degradation of sedimentary organic matter involves the use of Fe and Mn as secondary oxidants. The reduction of Fe and Mn results in their

Table 1 Correlation between sand, silt, clay, organic carbon (OC), metals, and pH of (a) core S9 and (b) core S17

	Sand	Silt	Clay	OC	Fe	Mn	Ni	Zn	Cr	Cu	Co	Pb	pH
Core S9 (a)													
Sand	1.00												
Silt	**−0.35**	1.00											
Clay	**−0.53**	**−0.61**	1.00										
OC	−0.07	0.12	−0.05	1.00									
Fe	0.22	−0.26	0.05	**−0.53**	1.00								
Mn	−0.07	0.02	0.04	0.15	−0.03	1.00							
Ni	**−0.39**	−0.03	**0.35**	−0.12	−0.09	**0.33**	1.00						
Zn	0.14	−0.24	0.10	**−0.35**	0.24	−0.05	0.23	1.00					
Cr	−0.06	**−0.31**	**0.33**	−0.17	0.24	**0.29**	**0.48**	**0.33**	1.00				
Cu	−0.02	−0.21	0.21	**−0.32**	**0.36**	0.09	**0.38**	**0.35**	**0.68**	1.00			
Co	−0.05	**−0.28**	**0.30**	−0.21	**0.39**	−0.02	0.17	0.22	**0.55**	**0.52**	1.00		
Pb	−0.20	−0.06	0.22	0.01	0.10	−0.13	0.19	0.03	0.01	0.00	0.24	1.00	
pH	−0.24	0.24	−0.01	**0.36**	**−0.39**	**0.46**	**0.49**	−0.20	0.07	−0.13	**−0.47**	−0.05	1.00
Core S17 (b)													
Sand	1.00												
Silt	**−0.61**	1.00											
Clay	**−0.70**	−0.13	1.00										
OC	**−0.45**	0.24	0.34	1.00									
Fe	0.15	−0.05	−0.15	−0.39	1.00								
Mn	−0.13	0.05	0.12	0.01	**0.76**	1.00							
Ni	−0.15	−0.13	0.30	−0.09	**0.82**	**0.85**	1.00						
Zn	0.16	−0.26	0.02	−0.29	**0.88**	**0.80**	**0.91**	1.00					
Cr	0.10	−0.33	0.16	−0.19	**0.82**	**0.80**	**0.92**	**0.91**	1.00				
Cu	−0.08	−0.19	0.27	−0.12	**0.83**	**0.82**	**0.99**	**0.93**	**0.94**	1.00			
Co	−0.13	−0.28	0.40	−0.02	**0.72**	**0.81**	**0.97**	**0.88**	**0.91**	**0.98**	1.00		
Pb	−0.34	−0.13	**0.55**	0.05	0.28	0.38	**0.57**	**0.43**	0.40	**0.61**	**0.68**	1.00	
pH	−0.17	−0.03	0.24	0.34	−0.31	−0.11	−0.34	−0.32	−0.23	−0.30	−0.22	−0.01	1.00

Numbers marked in bold are significant at $p < 0.05$

mobilization and upward diffusion to oxic surface sediments where they are reprecipitated either as oxides, or occasionally as carbonates (Farmer and Lovell 1984). The difference in peak depths further reflected the difference in oxidation kinetics of Fe^{+2} and Mn^{+3} (Zwolsman et al. 1993). However, Fe and Mn did not show significant positive correlation with each other in this core (Table 1a).

In core S17 (Fig. 3b) Fe concentration varies from 16.00 to 38.00 % (avg. 20) and Mn varies from 1,207 to 5,397 ppm (avg. 2,245). Not much variation in Fe and Mn concentration was noted from bottom to surface of the core except a prominent peak at 22 cm depth. Slightly higher values were also noted between 20 to 14 cm and 8 to 2 cm for Fe, while Mn showed an increase at the surface. The two metals showed large similarity in their distribution pattern between 36 and 6 cm depths. Unlike core S9, strong positive correlation (Table 1b) was noted between Fe and Mn indicating their association with each other in this core probably in the form of Fe–Mn oxyhydroxides.

Distribution of trace metals

In core S9 (Fig. 2b) the geochemical data shows a range of 216–267 ppm Ni (avg. 243), 208–460 ppm Zn (avg. 253), 198–320 ppm Cr (avg. 271), 308–422 ppm Cu (avg. 359), 91–149 ppm Co (avg. 111), 35–295 ppm Pb (avg. 67). Whereas, in core S17 (Fig. 3b) the geochemical data shows a range of 184–498 ppm Ni (avg. 217 ppm), 209–521 ppm Zn (avg. 253 ppm), 135–636 ppm Cr (avg. 271 ppm), 345–935 ppm Cu (avg. 403 ppm), 86–278 ppm Co (avg. 121 ppm), 17–128 ppm Pb (avg. 67 ppm). The elemental distribution within cores collected from the lower (core S9) and upper portions (core S17) of the middle estuary when compared showed less difference in their average concentrations. However, the range was observed to be wide in core S17 as compared to core S9 for Mn, Ni, Zn, and Cr.

In core S9, trace elements namely Zn, Cr, Cu, Co, and Pb showed an increasing trend from bottom up to 20 cm depth (Fig. 2b). This is followed by a decreasing trend till

4 cm and a slight increase towards the surface. While Ni showed higher values between 108 and 66 cm depth. Above 64 cm Ni showed an increasing trend up to 26 cm depth, this is followed by a decreasing trend towards the surface. The peak value obtained at 20 cm depth for Cr, Cu, and Co coincided with that of Mn, clay and organic carbon also. Similarly Ni, Cu, and Co peak at 26 cm and peak value of Ni and Pb at 98 cm coincided with that of Fe and organic carbon. Among trace elements, Ni, Zn, Cr, Cu, and Co showed a peak value at 68 cm depth. Correlation analyses indicated association of Ni, Cr, and Co with clay, while organic carbon also controlled the distribution of Ni, thus indicating the role of organic carbon and finer sediments in the distribution of some of the trace elements (De Groot et al. 1976; Salomons and Forstner 1984; Fletcher et al. 1994; Williams et al. 1994) in this core. Distribution of Cu and Co is similar to that of Fe, whereas Ni and Cr are associated with Mn and pH. Further, trace metals namely Ni, Zn, Cr, Cu, Co showed some correlation (Table 1a). The observed similarity in distribution trends of trace metals with that of Fe and Mn especially in the upper few centimeters, together with results of correlation matrix indicated association of trace metals with Fe–Mn oxyhydroxides in addition to clay and organic carbon as freshly formed Fe and Mn oxides are very efficient at scavenging a variety of heavy metals (Y-wu et al. 2010).

In core S17, all the analyzed trace elements showed similar trend to that of Fe and Mn (Fig. 3b). Metals maintained almost constant trend from bottom till the surface of the core except a prominent peak at 22 cm depth. Replicate analysis of the same sample to confirm the values gave similar readings. Slight increase in trace metal viz. Zn, Cr, and Co concentration at the surface similar to that of Mn was also evident, while a small peak value at 16 cm for Zn, Cu, and Co coincided with that of Fe and sand. Large similarity in distribution pattern of trace elements with that of Fe and Mn together with strong positive correlation between Fe, Mn, and all the studied trace metals except Pb indicated (Table 1b) that the distribution of heavy metals in this core was mainly controlled by the redox cycle of Fe and Mn (Chen et al. 2001). The distribution pattern pointed towards the co-precipitation of trace elements with Fe and Mn oxides. Further, the peak value obtained for all the elements at 22 cm depth coincided with that of clay. It is a known fact that the fine sediments associated with Fe/Mn oxyhydroxides together with organic coatings provide reactive sites for metal sorption (Grant and Middleton 1990; Cundy and Croudace 1995). However, among metals Pb showed strong positive correlation with clay, indicating difference in its distribution behavior and association.

Further, isocon plot was used to understand the variation of sediment components, organic carbon and studied metals at the two locations. Isocon plots allow an easy visual comparison of the average composition of each parameter (Grant 1986; Cundy et al. 1997; Rosales-Hoz et al. 2003). The results of the plotted data (Fig. 7) indicated the values of all the trace elements fall on the line. Thus, it can be inferred that there is no much variation in studied elemental average concentration between the two mudflat cores (S9 and S17). It also indicated less anthropogenic influence on trace metal distribution within Shastri estuary. Trace metals seem to be mainly derived from natural sources. However, Organic carbon and Mn fall towards core S17 indicating their association, while Fe points towards core S9 indicating different source for Mn and Fe.

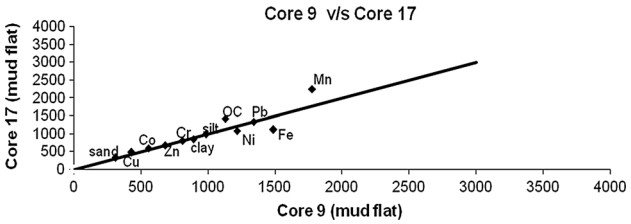

Fig. 7 Isocon diagram. Individual points represent average value of sediment component and elements

Index of geoaccumulation (I_{geo})

To evaluate the degree of pollution in sediments, geoaccumulation Index (I_{geo}) has been computed using the formula of Muller (1979) given below:

$$I_{geo} = \log_2(C_n/1.5 * B_n)$$

where I_{geo} is Index of geoaccumulation, C_n is measured concentration of element "n" and B_n is element content in "average shale" (Turekian and Wedepohl 1961) and the factor 1.5 is used because of possible variation of the background data due to lithogenic effects. Muller (1979) classified the level of pollution into seven classes based upon Index of geoaccumulation (I_{geo}) values viz "very strongly polluted"—I_{geo} class 6 ($I_{geo} > 5$); "Strong to very strong"—I_{geo} class 5 (I_{geo} 4–5); "Strongly polluted"—I_{geo} class 4 (I_{geo} 3–4); "Moderately to strongly polluted"—I_{geo} class 3 (I_{geo} 2–3); "Moderately polluted"—I_{geo} class 2 (I_{geo} 1–2); "Unpolluted to moderately polluted"—I_{geo} class 1 (I_{geo} 0–1) and "Unpolluted"—I_{geo} class 0 ($I_{geo} < 0$).

Average I_{geo} values for Shastri estuary showed different levels of pollution of metals (Muller 1979) within the sediments (Table 2, 3). Within sediments of core S9, Zn, and Mn fall under unpolluted to moderately polluted class. Fe, Ni, Cr, Co, and Pb represented moderately polluted class while Cu could be categorized under moderately to strongly polluted class. Same observation was true for core S17 except for Mn which fall under moderately polluted class. When the I_{geo} values of the two cores namely S17

Table 2 Geoaccumulation index

Pollution intensity	Sediment accumulation	I_{geo} class
Very strongly polluted	>5	6
Strongly to very strongly polluted	4–5	5
Strongly polluted	3–4	4
Moderately to strongly polluted	2–3	3
Moderately polluted	1–2	2
Unpolluted to moderately polluted	0–1	1
Practically unpolluted	<0	0

Table 3 Average I_{geo} values

Core	Mn	Fe	Ni	Zn	Cr	Cu	Co	Pb
S9	0.9	2.0	1.3	0.8	1.1	2.4	2.0	1.1
S17	1.3	1.5	1.0	0.8	1.1	2.6	2.0	1.1

and S9 were compared, all the metals showed same level of enrichment within the two cores except Mn. Mn showed difference in level of pollution at the two locations. Mn enrichment was one level higher towards the upper middle estuary indicating enhanced supply of Mn probably from the catchment area. The additional supply can be due to change in land use–land cover in the recent years.

Metal speciation in sediments

To know the processes governing metal accumulation and bioavailability, speciation study was carried on redox sensitive Fe and Mn together with trace metal Co. The results are diagrammatically represented in the Fig. 8.

Iron (Fe) Fe in residual fraction ranges from 11.71 to 16.30 % (avg. 15.04) which accounts for 90.14–96.01 % when recomputed taking all five fractions to 100 in core S9. In core S17, Fe ranges from 13.45 to 17.59 % (avg. 15.72) and accounts for 91.99–94.14 %. Next to residual fraction, Fe is mainly bound to Fe–Mn oxides fraction, which ranges from 4890 to 12,203 ppm (avg. 7,250) and accounts for 2.88–7.99 % in core S9. In core S17, it ranges from 7,703 to 11,358 ppm (avg. 9,414) which accounts for 4.39–6.49 %. Iron concentration in exchangeable fraction ranges from 0.78 to 2.00 ppm (avg. 1.24) in core S9 and 1.00–38.00 ppm (avg. 13.76) in core S17. In Carbonate bound fraction it varies from 6.00 to 135.00 ppm (avg. 35.02) in core S9 and 11.00–17.00 ppm (avg. 13.75) in core S17. In the organic bound fraction Fe ranges from 1,110 to 2,645 ppm (avg. 1,900) in core S9 and 1,533–4,830 ppm (avg. 2,586) in core S17.

Fe concentration was very less in the bioavailable phases, i.e., exchangeable, carbonate bound, Fe–Mn oxide and organic bound fractions added together. Major quantity of Fe was found to be associated with the residual fraction in both the cores (Fig. 8a). Metals in this phase mostly remain stable and do not react during sedimentation and diagenesis and, therefore, have less potential bioavailability. Therefore, this phase was considered as inert phase corresponding to the part of metal that cannot be mobilized (Tessier et al. 1979).

Manganese (Mn) Mn ranges from 780 to 1,200 ppm (avg. 977) in the residual fraction which accounts for 28.94–89.46 % when recomputed taking all five fractions to 100 in core S9. While in core S17 Mn ranges from 875 to 1,455 ppm (avg. 1,075) which accounts for 23.41–54.79 %. Next to residual fraction, Mn is mainly bound to carbonate fraction in core S9 and to exchangeable and Fe–Mn oxides fractions in core S17. In core S9, Mn in the carbonate fraction ranges from 14 to 1,816 ppm (avg. 371) which accounts for 1.00–61.34 %. In core S17 exchangeable Mn varies from 251 to 2,678 ppm (avg. 1,234) which accounts for 10.27–71.44 % and Mn in Fe–Mn oxide fraction varies from 47 to 1,544 ppm (avg. 444) which accounts for 1.27–45.20 %. Mn concentration (ppm) in exchangeable, Fe–Mn oxide and organic bound fraction ranges from 62 to 534 (avg. 273), 2.85 to 118 (avg. 47) and 1.23 to 67 (avg. 17), respectively, in core S9. Whereas in case of core S17 carbonate bound Mn varies from 1 to 136 ppm (avg. 43) and organic bound Mn it varies from 39 to 106 ppm (avg. 67).

Considerably higher amount of Mn was present in the bioavailable phases in both the cores (Fig. 8b). The higher level of Mn in carbonate fraction in core S9 is most likely due to the similarity in ionic radii of Mn to that of calcium that allows Mn to substitute for calcium in carbonate phase (Pederson and Price 1982; Zhang et al. 1988). While the higher concentration of Mn in exchangeable fraction in core S17 indicates weakly bound Mn, it is considered to be the most unstable and reactive phase (Passos et al. 2010). Further, the mechanism of Mn accumulation within reducible fraction may be related to precipitation and co-precipitation with Fe–Mn oxides (Li et al. 2001).

As evident from the Fig. 8b, association of Mn with sedimentary fractions is different in the two cores. In core S9, higher percentage of carbonate relative to exchangeable bound Mn is present at greater depths and vice versa towards the shallower depths. The loosely bound exchangeable fraction towards the surface is probably derived from recent anthropogenic activities. In core S17, Mn associated with exchangeable fraction decreased and that associated with residual fraction increased from bottom to 14 cm depth. While towards the surface of the core increase in Fe–Mn oxide bound fraction is noted. Both the cores showed lower residual bound Mn concentration

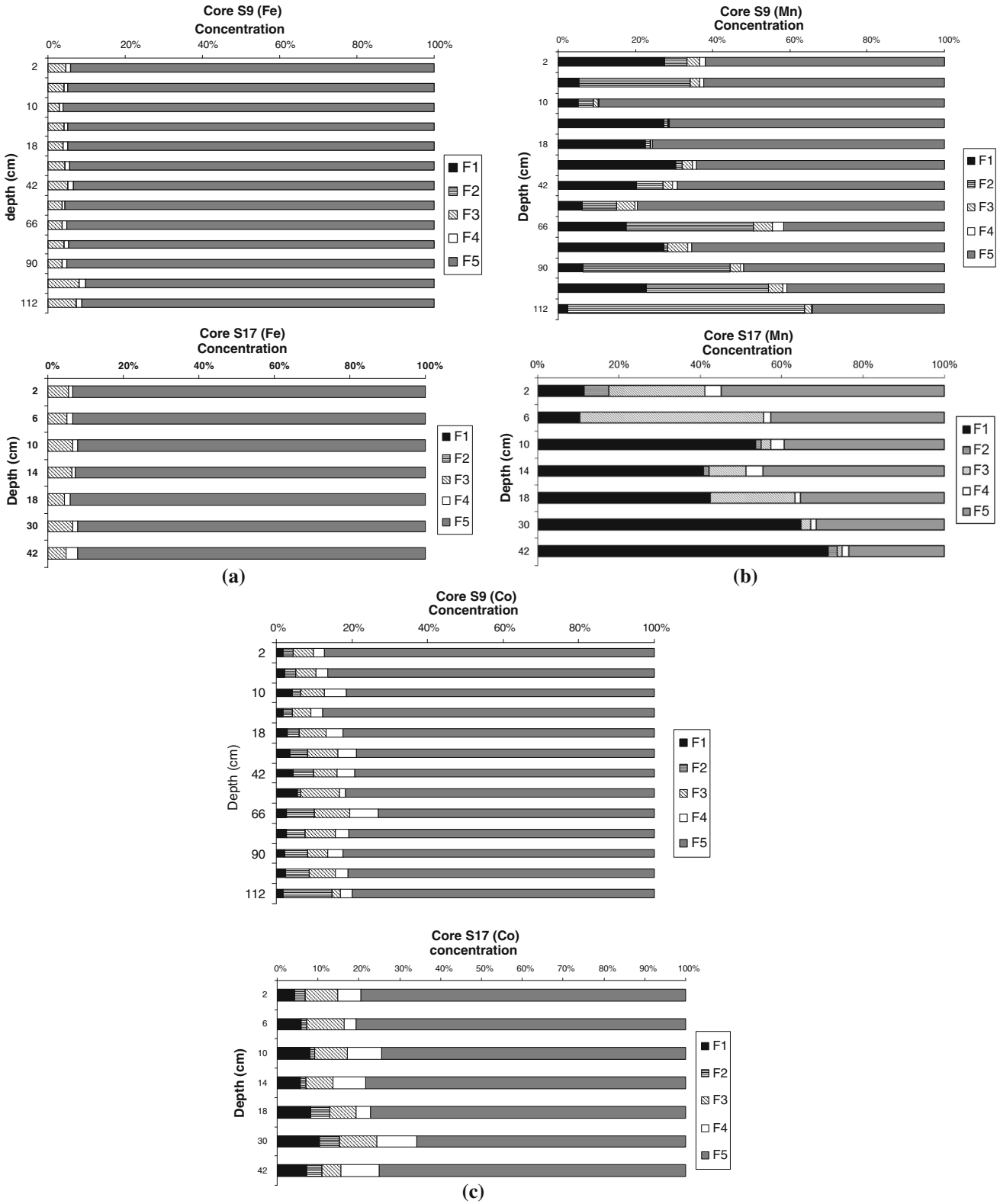

Fig. 8 Extractable contents of **a** Fe, **b** Mn, and **c** Co in Tessier sequential extraction protocol for the mudflats cores S9 and S17. F1 exchangeable fraction, F2 carbonate bound fraction, F3 Fe–Mn oxide fraction, F4 organic/sulfide bound fraction, F5 residual fraction

towards the greater depths. This distribution pattern probably indicates dilution of loosely bound labile fractions of Mn by land-derived terrestrial material in recent past (Qi et al. 2010). However, increased Mn concentration in reactive phases at the surface indicates anthropogenic addition. Normally, "exchangeable and carbonate" bound fractions are considered to be most labile and metals associated with these fractions become mobile in the case of environmental changes (Charriau et al. 2011). Both the cores have shown higher concentration of bioavailable fraction towards the bottom. Reductive dissolution of Fe–Mn hydroxides in the suboxic zone can release dissolved Mn (II) and Fe (II) to pore waters, potentially making them more bioavailable and mobile (Koretsky et al. 2007). It also suggests a decrease in potential for remobilization of metals in recent years except at the surface. However, if sediments are reworked by process of bioturbaton or human interference like dredging, else a change in pH, redox conditions or degradation of organic matter can lead to release of Mn at the sediment water interface that is into the estuarine environment, causing a potential risk of toxicity to the organisms.

Cobalt (Co) The concentration of Co in the residual fraction ranges from 39.00 to 59.00 ppm (avg. 51.59) which accounts for 72.89–87.75 % in core S9 (Fig. 8c) and 29.00–52.00 ppm (avg. 41.73) which accounts for 65.89–80.60 % in core S17 when recomputed taking all five fractions to 100. In core S9, Co ranges from 1.00 to 6.00 ppm (avg. 4.13) in the Fe–Mn oxide fraction and accounts for 2.23–10.38 %. In core S17, Co varies from 3.00 to 5.00 ppm (avg. 4.03) in Fe–Mn oxide fraction and accounts to 4.82–9.27 %, in exchangeable fraction Co varies from 2.00 to 5.00 ppm (avg. 3.81) which accounts for 4.36–10.29 % and in organic bound fraction it varies from 1.70 to 6.50 ppm (avg. 3.77) and accounts for 2.96–9.66 %. Co concentration in exchangeable fraction ranges from 1.00 to 3.50 ppm (avg. 1.86), in carbonate bound fraction it ranges from 0.60 to 7.00 ppm (avg. 2.89) and in organic bound fraction it varies from 1.00 to 4.00 ppm (avg. 2.52) in core S9. Whereas in core S17 in carbonate bound fraction Co varies from 0.70 to 2.50 ppm (avg. 1.51).

Highest concentration of Co was found to be associated with the residual fraction of sediments. Bioavailable fraction of Co showed a decreasing trend while Co associated with residual fraction showed a general increasing trend towards the surface of both the cores. Thus, pointing towards increased addition of Co associated with weathered terrestrial source material which causes reduction in mobility of Co in recent years.

Risk assessment

When the average total metal concentration in sediments (Table 4) was compared with SQUIRT's table (Table 6), Mn, Co, Ni, and Cr values exceeded the apparent effect threshold (AET) in both the cores whereas Fe and Cu concentrations were above AET in core S9 and S17, respectively. However, in core S9, Cu concentration exceeded ERM. Zn and Pb concentrations were below PEL in the two cores. Thus, among the studied metals only Zn and Pb are relatively less harmful, while all the other metals indicate high risk of toxicity and adverse effect on the biota (Buchman 1999). Due to differences in metal partitioning behavior, considerable percentages of metals are associated with less reactive residual fraction. Therefore, even though total metal concentrations are much higher, the analysis of the total metal data may not reflect, accurately, potential bioavailability in these sediments. Thus, concentrations of selected metals (Fe, Mn, and Co) extracted during stages 1–4 of the sequential extraction scheme were considered. Here, Mn was found to be mainly associated with bioavailable fractions (sum of first four fractions) and, therefore, indicates anthropogenic origin. Mn in bioavailable fraction (Table 5) exceeded AET, therefore, suggesting a high risk of toxicity (Tables 6, 7). Fe and Co were mainly bound to the residual fraction and represented metals of natural origin. Also, the percentage of Fe was very low compared to AET indicating no harm. However, Co associated with bioavailable fractions exceeded the AET (Tables 4, 5) suggesting risk of toxicity of Co to organisms associated with the sediments of Shastri estuary.

Conclusions

The study carried out in the middle estuary revealed that the sediments of the upper middle estuary show signatures of variation in hydrodynamic condition and the tributary is responsible for the addition of higher organic carbon and metal concentrations. Relatively higher concentration of Mn in bioavailable phases in the upper middle estuary is

Table 4 Average total concentration of metals in the two mudflat cores

Core	Mn (ppm)	Fe (%)	Ni (ppm)	Zn (ppm)	Cr (ppm)	Cu (ppm)	Co (ppm)	Pb (ppm)
S9	1,778	27	243	253	271	359	111	67
S17	2,245	20	217	253	271	403	121	67

Table 5 Total concentration of metals and bioavailable fractions in the two mudflat cores

Metals	Range	Lower middle estuary (S9)		Upper middle estuary (S17)	
		Total metal conc. ppm	Bioavailable fraction (F1 + F2 + F3 + F4) ppm	Total metal conc. ppm	Bioavailable fraction (F1 + F2 + F3 + F4) ppm
Fe	Min	205,563	6,770	157,098	10,354
	Max	370,176	14,803	381,625	13,634
	Avg	270,783	9,186	202,924	12,027
Mn	Min	1,133	126	1,206	996
	Max	2,823	1,947	5,396	2,871
	Avg	1,778	707	2,244	1,787
Co	Min	90	8.25	86	10.97
	Max	149	14.32	278	17.3
	Avg	111	11.40	120	13.11

Table 6 Screening quick reference table (SQUIRT) for metals in marine sediments (Buchman 1999)

Elements	Threshold effect level (TEL)	Effects range low (ERL)	Probable effects level (PEL)	Effects range median (ERM)	Apparent effects threshold (AET)
Fe	–	–	–	–	22 % (Neanthes)
Mn	–	–	–	–	260 (Neanthes)
Ni	15.9	20.9	42.8	51.6	110 (Echinoderm larvae)
Zn	124	150	271	410	410 (Infaunal community)
Cr	52.3	81	160.4	370	62 (Neanthes)
Cu	18.7	34	108.2	270	390 (Microtox and oyster larvey)
Co	–	–	–	–	10 (Neanthes)
Pb	30.24	46.7	112.18	218	400 (Bivalve)

Table 7 Sediment guidelines and terms used in SQUIRT

Threshold effect level (TEL)	Maximum concentration at which no toxic effects are observed
Effects range low (ERL)	10th percentile values in effects or toxicity may begin to be observed in sensitive species
Probable effects level (PEL)	Lower limit of concentrations at which toxic effects are observed
Effects range median (ERM)	50th percentile value in effects
Apparent effects threshold (AET)	Concentration above which adverse biological impacts are observed

related to increased addition of material from anthropogenic sources. While the elevated concentration of Fe and Co in the residual fraction indicated their natural lithogenic source. Further, Mn and Co exceeded the apparent threshold level at both the locations indicating their toxicity to the environment of Shastri estuary.

Acknowledgments One of the authors (GNN) wish to thank the Ministry of Earth Sciences, New Delhi for the financial support to carry out research work on mudflats along central west coast of India.

References

Achuthankutty CT, Nair SRS, Devassy VP, Nair VR (1981) Plankton composition in two estuaries of the Konkan coast during premonsoon season. Mahasagar—Bull Natl Inst Oceanogr 14(1):55–60

Allen GP, Posamentier HW (1993) Sequence stratigraphy and facies model of an incised valley fill: the Gironde estuary. Fr J Sediment Pet 63(3):378–391

Almas AR, Lombnaes P, Sogn TA, Mulder J (2006) Speciation of Cd and Zn in contaminated soils assessed by DGT-DIFS, and WHAM/MODEL VI in relation to uptake by spinach and ryegrass. Chemosphere 62:1647–1655

Attri K, Kerkar S (2011) Seasonal assessment of heavy metal pollution in tropical mangrove sediments (Goa, India). J Ecobiotech 3(8):09–15

Boyes SJ, Allen JH (2007) Topographic monitoring of a middle estuary mudflat, Humber estuary, UK—anthropogenic impacts and natural variation. Mar Pollut Bull 55:543–554

Buchman MF (1999) NOAA screening quick reference tables. NOAA HAZMAT report 99–111, Coastal Protection and Restoration Division, National Oceanic and Atmospheric administration, Seattle, WA, p 12

Charriau A, Lesven L, Gao Y, Leermakers M, Baeyens W, Ouddane B, Billon G (2011) Trace metal behaviour in riverine sediments: role of organic matter and sulfides. Appl Geochem 26: 80–90

Chen Z, Liu P, Xu S, Liu L, Yu J, Yu L (2001) Spatial distribution and accumulation of heavy metals in tidal flat sediments of Shanghai coastal zone. Sci China Ser B Chem 44(1):197–208

Cundy AB, Croudace IW (1995) Physical and chemical associations of radionuclides and trace metals in estuarine sediments; an example from Poole harbour, southern England. J Environ Radioact 29:191–212

Cundy AB, Croudace IW, Thomson J, Lewis JT (1997) Reliability of salt marshes as 'geochemical recorders' of pollution input: a case study from contrasting estuaries in Southern England. Environ Sci Technol 31:1093–1101

Dalrymple RW, Zaitlin BA, Boyd R (1992) Estuarine facies models: conceptual basis and stratigraphic implications. J Sediment Pet 62(6):1130–1146

Davies JL (1964) A morphogenic approach to world shoreslines: zeitschrift Fur Geomorphologie. Band 8:27–42

De Groot AJ, Salomons W, Allersma E (1976) Processes affecting heavy metals in estuarine sediments. In: Burton JD, Liss PS (eds) Estuar Chem. Academic Press, London, pp 131–157

Delacerd LD (1983) Heavy metal accumulation by mangrove salt marsh intertidal sediments. Braz J Med 16:442–451

Dessai DVG, Nayak GN (2009) Distribution and speciation of selected metals in surface sediments, from the tropical Zuari estuary, central west coast of India. Environ Monit Assess 158:117–137

Fairbridge RW (1980) The estuary: its definition and geodynamic cycle. In: Olausson E, Cato I (eds) Chemistry and biogeochemistry of estuaries. Wiley, New York, pp 1–35

Farmer JG, Lovell MA (1984) Massive diagenetic enhancement of manganese in loch lomond sediments. Environ Technol Lett 5:257–262

Fernandes L, Nayak GN (2009) Distribution of sediment parameters and depositional environment of mudflats of Mandovi estuary, Goa India. J Coast Res 25(2):273–284

Fernandes L, Nayak GN (2012a) Geochemical assessment in a creek environment: Mumbai, west coast of India. Environ Forensics 3:45–54

Fernandes L, Nayak GN (2012b) Heavy metals contamination in mudflat and mangrove sediments (Mumbai, India). Chem Ecol 28(5):435–455

Fernandes L, Nayak GN, Ilangovan D, Borole DV (2011) Accumulation of sediment, organic matter, and trace metals with space and time, in a creek along Mumbai coast, India. Estuar Coast Shelf Sci 91:388–399

Fletcher CA, Bubbs JM, Lester JN (1994) Magnitude and distribution of contaminants in five salt marshes on the Essex coast, United Kingdom I. Addressing the problem, site description and physico-chemical parameters. Sci Total Environ 155:312–345

Folk RL (1968) Petrology of sedimentary rocks. Austin, Hemphills, p 177

Francois R (1988) A study on regulation of the concentrations of some trace metals (Rh, Sr, Zn, Pb, Cu, V, Cr, Ni, Mn, and Mo) in saanich inlet sediments, British Columbia, Canada. Mar Geol 83:285–308

Grant JA (1986) The isocon diagram—a simple solution to gresen's equation for metasomatic alteration. Econ Geol 81:1976–1982

Grant SH, Middleton R (1990) An assessment of metal contamination of sediments in the Humber estuary. UK Estuar Coast Shelf Sci 31:71–85

Harbison P (1986) Mangrove muds—a sink and source for trace metals. Mar Pollut Bull 17:246–250

Hu XF, Du Y, Feng JW, Fang SQ, Gao XJ, Xu SY (2013) Spatial and seasonal variations of heavy metals in wetland soils of the tidal flats in the Yangtze estuary, china, environmental implications. Pedosphere 23(4):511–522

Jackson ML (1958) Soil chemical analysis. Prentice-Hall, New York

Jones B, Turki A (1997) Distribution and speciation of heavy metals in surfacial sediments from the Tees estuary, north-east England. Mar Pollut Bull 34(10):768–779

Klavinš M, Briede A, Rodinov V, Kokorite I, Parele E, Klavina I (2000) Heavy metals in rivers of Latvia. Sci Total Environ 262:175–184

Koretsky CM, Haveman M, Beuving L, Cuellar A, Shattuck T, Wagner M (2007) Spatial variation of redox and trace metal geochemistry in a minerotrophic fen. Biogeochemistry 86:33–62. doi:10.1007/s10533-007-9143-x

Kumar SP, Edward JKP (2009) Assessment of metal concentration in the sediment cores of Manakudy estuary, south west coast of India. Indian J Mar Sci 38(2):235–248

Kumaran KPN, Shindikar M, Limaye RB (2004) Mangrove associated lignite beds of Malvan, Konkan: evidence for higher sea level during the late tertiary (Neogene) along the west coast of India. Curr Sci 86(2):335–340

Lesueur P, Lesourd S, Lefebvre D, Garnaud S, Brun-Cottan JC (2003) Holocene and modern sediments in the Seine estuary (France): a synthesis. J Quat Sci 18(3–4):339–349

Li X, Shen Z, Wai OWH, Li Y-S (2001) Chemical forms of Pb, Zn, and Cu in the sediment profiles of the Pearl river estuary. Mar Pollut Bull 42(3):215–223

Marchand C, Lallier-Verges E, Baltzer F, Alberic P, Cossa D, Baillif P (2006) Heavy metals distribution in mangrove sediments along the mobile coastline of French Guiana. Mar Chem 98:1–17

Mayer LM, Xing BS (2001) Organic matter–surface area relationships in acid oils. Soil Sci Am J 65:250–258

McCaffrey RJ, Thomson J (1980) A record of the accumulation of sediments and trace metals in a Connecticut, USA, salt marsh. Adv Geophys 22:165–236

Muller G (1979) Schwermetalle in den Sedimentation des Rheins–Ver-anderungen seit 1971. Umschau 79:778–783

Nair CK, Balachand AN, Chacko J (1993) Sediment characteristics in relation to changing hydrography of Cochin estuary. Indian J Mar Sci 22:33–36

Pande A, Nayak GN (2013a) Understanding distribution and abundance of metals with space and time in estuarine mudflat sedimentary environment. Environ Earth Sci. doi:10.1007/s12665-013-2298-y

Pande A, Nayak GN (2013b) Depositional environment and preferential site of metal concentration in mudflats of dharamtar creek, west coast of India. Indian J Geo-Marine Sci 42(3):360–369

Passos EA, Alves JC, Santos IS, Alves JPH, Garcia CAB, Costa ACS (2010) Assessment of trace metals contamination in estuarine sediments using a sequential extraction technique and principal component analysis. Microchem J 96:50–57

Pederson TF, Price NB (1982) The geochemistry of manganese carbonate in panama basin sediments. Geochim Cosmochim Acta 46(1):59–68

Pejrup M (1988) The triangular diagram used for classification of estuarine sediments: a new approach. In: de Boer PL, van Gelder A, Nios SD (eds) Tide–influenced sedimentary environments and facies. Reidel, Dordrecht, pp 289–300

Qi S, Leipe T, Rueckert P, Di Z, Harff J (2010) Geochemical sources, deposition and enrichment of heavy metals in short sediment cores from the Pearl river estuary, Southern China. J Marine Syst 82:28–42

Rajamanickam GV, Gujar AR (1995) Transparent heavy mineral distribution in the bays of Jaigad, Ambwah, and Varvada, Ratnagiri district Maharashtra. J Indian Assoc Sedimentol 14:43–53

Reineek HE (1972) Tidal flats. In: Rigby JK, Hamblin WK (eds) Recognition of Ancient Sedimantary Environments, Tulsa, Okla. Soc Econ Paleontol Mineral Spec Publ 16:146–159

Rosales-Hoz L, Cundy AB, Bahena–Manjarrez JL (2003) Heavy metals in sediment cores from a tropical estuary affected by anthropogenic discharges: Coatzacoalcos estuary, Mexico. Estuar Coast Shelf Sci 58:117–126

Salomons W, Forstner U (1984) Metals in hydrosphere. Springer, Berlin, p 349

Singh J (2013) 2012 Port Information & Policy, JSW Jaigarh Port. http://www.jsw.in/infrastructure/pdfs/download/jaigarh/JSWJPL%20Port%20Rules%20Rev0.pdf

Singh KT, Nayak GN (2009) Sedimentary and geochemical signatures of depositional environment of sediments in mudflats from a microtidal Kalinadi estuary, central west coast of India. J Coastal Res 25(3):641–650

Singh KT, Nayak GN, Fernandes LL (2012) Geochemical evidence of anthropogenic impacts in sediment cores from mudflats of a tropical estuary, Central west coast of India. Soil Sediment Contam 22(3):256–272

Singh KT, Nayak GN, Fernandes LL, Borole DV, Basavaiah N (2013) Changing environmental conditions in recent past—Reading through the study of geochemical characteristics, magnetic parameters and sedimentation rate of mudflats, central west coast of India. Palaeogeogr Palaeoclimatol Palaeoecol. http://dx.doi.org/10.1016/j.palaeo.2013.04.008

Siraswar R, Nayak GN (2011) Mudflats in lower middle estuary for concentration of metals. Indian J Mar Sci 40(3):372–385

Soto-Jime′nez MF, Pa′ez-Osuna F (2001) Cd, Cu, Pb, and Zn in lagoonal and mangrove sediments from Mazatla'n port (SE Gulf of California): geochemical associations and bioavailability. Bull Environ Contam Toxicol 66:350–356

Spencer KL, Macleod CL (2002) Distribution and partitioning of heavy metals in estuarine sediment cores and implications for the use of sediment quality standards. Hydrol Earth Syst Sc 6(6):989–998

Spencer KL, Cundy AB, Croudace IW (2003) Heavy metal distribution and early diagenesis in salt marsh sediments from the Medway estuary, Kent, UK. Estuar Coast Shelf Sci 57:43–54

Statsoft (1999) Statistica computer programme, version 5.5. StatSoft, Tulsa, OK

Szefer P, Glassby GP, Pempkowiak J, Kaliszan R (1995) Extraction studies of heavy metal pollutants in surficial sediments from the southern baltic sea off Poland. Chem Geol 120(1–2):111–126

Tam NFY, Wong YS (2000) Spatial variation of heavy metals in surface sediments of Hong Kong mangrove swamps. Environ Pollut 110(2):195–205

Tessier A, Campbell PGC, Bisson M (1979) Sequential extraction procedure for the speciation of particulate trace metals. Anal Chem 51(7):844–851

Thomas CA, Bendell-Young LI (1998) Linking the sediment geochemistry of an intertidal region to metal bioavailability in the deposit feeder Macoma balthica. Mar Ecol Prog Ser 173:197–213

Turekian KK, Wedepohl KH (1961) Distribution of the elements in some major units of the earth's crust. Geol Soc Am Bull 72:175–192

Volvoikar SP, Nayak GN (2013a) Depositional environment and geochemical response of mangrove sediments from creeks of northern Maharashtra coast, India. Mar Pollut Bull 69:223–227

Volvoikar SP, Nayak GN (2013b) Evaluation of impact of industrial effluents on intertidal sediments of a creek. Int J Environ Sci Technol 10(5):941–954

Volvoikar SP, Nayak GN (2013c) Factors controlling the distribution of metals in intertidal mudflat sediments of Vaitarna estuary, North Maharashtra coast, India. Arab J Geosci. doi:10.1007/s12517-013-1162-4

Walkey-Black A (1947) A critical examination of a rapid method for determining organic carbon in soil. Soil Sci 63:251–263

Welle BA, Hirsch AC, Davis LE, Johnson AC, Hunt GJ, Eves RL (2004) Origin of calcareous sediments in the Holocene Pigeon Creek Tidal lagoon and tidal delta, San Salvador Island, Bahamas. Am J Undergrad Res 3(1):1–8

Wells JT, Coleman JM (1981) Periodic mudflat progradation, northeastern coast of South America: a hypothesis. J Sediment Petrol 51:1069–1075

Williams TP, Bubb JM, Lester JN (1994) Metal accumulation within salt marsh environments: a review. Mar Pollut Bull 28:277–290

Wu Z, He M, Lin C, Fan Y (2011) Distribution and speciation of four heavy metals (Cd, Cr, Mn, and Ni) in the surficial sediments from estuary in daliao river and yingkou bay. Environ Earth Sci 63:163–175

Zhou YW, Zhao B, Peng YS, Chen GZ (2010) Influence of mangrove reforestation on heavy metal accumulation and speciation in intertidal sediments. Mar Pollut Bull 60:1319–1324

Zhang J, Huang WW, Martin JM (1988) Trace metals distribution in Huanghe (Yellow River) estuarine sediments. Estuar Coast Shelf Sci 26:499–526

Zwolsman JJG, Berger GW, Van Eck GTM (1993) Sediment accumulation rates, historical input, post- depositional mobility and retention of major elements and trace elements in salt marsh sediments of the Scheldt estuary, SW Netherlands. Mar Chem 44:73–94